American Heart Association.
Circulation
Manuscript Submission and Peer Review System

Disclaimer: The manuscript and its contents are confidential, intended for journal review purposes only, and not to be further disclosed.

URL: http://circ-submit.aha-journals.org

Title: Targeting chondroitin sulphate glycosaminoglycans to treat cardiac fibrosis in pathological cardiac remodelling

Manuscript number: CIRCULATIONAHA/2017/030353R2

Author(s): Roger Foo, Genome Institute of Singapore
Rongrong Zhao, National University of Singapore
Matthew Ackers-Johnson, National University of Singapore
Justus Stenzig, University Medical Center Hamburg-Eppendorf
Chen Chen, National University of Singapore
Tao Ding, National University of Singapore
Yue Zhou, National University of Singapore
Peipei Wang, National University of Singapore
Shi Ling Ng, Genome Institute of Singapore
Peter Li, National University of Singapore

Gavin Teo, Bioprocessing Technology Institute

Pauline Rudd, NIBRT

JW Fawcett, Centre for Brain Repair

Disclaimer: The manuscript and its contents are confidential, intended for journal review purposes only, and not to be further disclosed.

Targeting chondroitin sulfate glycosaminoglycans to treat cardiac fibrosis in pathological remodeling

Rong-Rong Zhao[1], Matthew Ackers-Johnson[1], Justus Stenzig[2,3], Chen Chen[4], Tao Ding[1], Zhou Yue[1], Wang Peipei[1], Shi Ling Ng[2], Peter Y. Li[1], Gavin Teo[4], Pauline M Rudd[4,5], James W. Fawcett[6], Roger S.Y. Foo[1,2]*

[1]Cardiovascular Research Institute, National University of Singapore, Singapore

[2]Genome Institute of Singapore, Agency for Science, Technology and Research, Singapore

[3]Department of Experimental Pharmacology and Toxicology, University Medical Center Hamburg-Eppendorf, Hamburg, Germany

[4]Bioprocessing Technology Institute, Agency for Science, Technology and Research, Singapore

[5]Glycoscience Group, National Institute for Bioprocessing, Research and Training, Dublin, Ireland

[6]John van Geest Centre for Brain Repair, University of Cambridge, UK

*Corresponding author

Roger Foo

Genome Institute of Singapore

60 Biopolis Street

Singapore 138672

Tel: +65-6808 8232

Fax: +65-6872 2998

Email: foosyr@gis.a-star.edu.sg

Disclaimer: The manuscript and its contents are confidential, intended for journal review purposes only, and not to be further disclosed.

1 Symbols, abbreviations and acronyms:

AB	Alcian blue
ASB	arylsulfatase B
CF	cardiac fibroblast
chABC	chondroitinase ABC
CI	colloidal iron
CS	chondroitin sulfate
CSPG	chondroitin sulfate proteoglycan
DS	dermatan sulfate
EC	endothelial cell
ECM	extracellular matrix
ERT	enzyme replacement therapy
EsCM	end-stage cardiomyopathy
GAG	glycosaminoglycan
HA	hyaluronic acid
HAS	human serum albumin
HF	heart failure
HS	heparan sulfate
IL	interleukin
LCMS	liquid chromatography mass spectrometry
LV	left ventricular
mAb	monoclonal antibody
MPS	mucopolysaccharidosis
MW	molecular weight
Mφ	macrophage
PG	proteoglycan
PMA	phorbol myristate acetate
rhASB	recombinant human arylsulfatase B

Disclaimer: The manuscript and its contents are confidential, intended for journal review purposes only, and not to be further disclosed.

SD	standard deviation
SLRP	small leucine-rich proteoglycan
SPR	surface plasmon resonance
SR	Sirius red
SMC	smooth muscle cell
TBH	tert-butyl hydroperoxide
TGFβ	transforming growth factor β
TNFα	tumor necrosis factor α

1

Disclaimer: The manuscript and its contents are confidential, intended for journal review purposes only, and not to be further disclosed.

Abstract:

Background: Heart failure (HF) is a leading cause of mortality and morbidity, and the search for novel therapeutic approaches continues. In the monogenic disease mucopolysaccharidosis (MPS) VI, loss of function mutations in arylsulfatase B leads to myocardial accumulation of chondroitin sulfate (CS) glycosaminoglycans (GAGs), manifesting as a myriad of cardiac symptoms. Here, we studied changes in myocardial CS in non-MPS failing hearts, and assessed its generic role in pathological cardiac remodeling.

Methods: Healthy and diseased human and rat left ventricles were subjected to histological and immuno-staining methods to analyze for GAG distribution. GAGs were extracted and analyzed for quantitative and compositional changes using Alcian Blue assay and liquid chromatography mass spectrometry. Expression changes in 20 CS-related genes were studied in three primary human cardiac cell types and THP-1 derived macrophages under each of 9 *in vitro* stimulatory conditions. In two rat models of pathological remodeling induced by transverse aortic constriction (TAC) or isoprenaline infusion, recombinant human arylsulfatase B (rhASB), clinically used as enzyme replacement therapy in MPS VI, was administered intravenously for 7 or 5 weeks respectively. Cardiac function, myocardial fibrosis and inflammation were assessed by echocardiography and histology. CS-interacting molecules were assessed using surface plasmon resonance and a mechanism of action was verified *in vitro*.

Results: Failing human hearts displayed significant perivascular and interstitial CS accumulation, particularly in regions of intense fibrosis. Relative composition of CS disaccharides remained unchanged. TGFβ induced CS upregulation in cardiac fibroblasts. CS accumulation was also observed in both the pressure-overload and the isoprenaline models of pathological remodeling in rats. Early treatment with rhASB in the TAC model, and delayed treatment in the isoprenaline model, proved rhASB to be effective at preventing cardiac deterioration and augmenting functional recovery. Functional improvement was accompanied by reduced myocardial inflammation and overall fibrosis. TNFα was identified as a direct binding partner of CS GAG chains, and rhASB reduced TNFα-induced inflammatory gene activation *in vitro* in endothelial cells and macrophages.

Disclaimer: The manuscript and its contents are confidential, intended for journal review purposes only, and not to be further disclosed.

Conclusions: CS GAGs accumulate during cardiac pathological remodeling, and mediate myocardial inflammation and fibrosis. RhASB targets CS effectively as a novel therapeutic approach for the treatment of heart failure.

Clinical Perspective

What Is New?

- Failing human hearts display an abundant accumulation of chondroitin sulfate proteoglycans (CSPG) in the extracellular matrix, largely localized to fibrotic regions.
- The main component of CS glycosaminoglycan (GAG) chains in CSPGs in human hearts is chondroitin-4-sulfate (C4S).
- TNFα is a direct binding partner of GAG chains rich in C4S.
- Modification of the CS chain with the recombinant human arylsulfatase B (rhASB), an FDA-approved treatment for Mucopolysaccharidosis type VI targeting C4S, reduces myocardial inflammation and overall fibrosis *in vivo*.
- In 2 independent rodent models of pathological cardiac remodelling, rhASB treatment prevented cardiac deterioration and improved functional recovery.

What Are the Clinical Implications?

- Targeting ECM CS represents a novel therapeutic approach for the treatment of heart failure.

Disclaimer confidential only

Introduction

The failing heart undergoes extensive extracellular matrix (ECM) remodeling during disease progression. ECM contains structural components such as collagen, as well as non-structural components comprising of glycoproteins, proteoglycans (PGs), and glycosaminoglycans (GAGs).[1, 2] Changes in ECM components are involved in important aspects of pathological cardiac remodeling such as the regulation of inflammation and fibrosis.[2-5] PGs are composed of a protein core to which one or more GAG chains are attached. GAGs are unbranched polysaccharides including chondroitin sulfate (CS), dermatan sulfate (DS), heparan sulfate (HS), heparin and hyaluronic acid (HA). CS / DS and HS are highly sulfated, and are therefore among the most negatively-charged of all naturally occurring high molecular weight biomolecules.

A group of rare diseases known as mucopolysaccharidosis (MPS) I-VII exhibits systemic GAG accumulation caused by gene mutations in GAG degradation enzymes. MPS patients suffer from progressive GAG deposition and multi-organ dysfunction, among which cardiac symptoms are common and early-onset.[6] Myocardial GAG accumulation manifests as ventricular fibrosis, hypertrophy, arrhythmia, valve leaflet disease, and in some cases ventricular aneurysm.[6, 7] MPS VI is specifically caused by loss of function mutations in the gene encoding the arylsulfatase B (ASB) enzyme, leading to the accumulation of N-acetylgalactoseamine-4S, a component of the major CS subtype C4S, and DS. Enzyme replacement therapy for MPS VI patients with recombinant human ASB (rhASB) significantly reduces ventricular dysfunction in young patients,[8] and early treatment prevents abnormal cardiac development.[9]

In non-MPS individuals, aging and ischemic injury also result in myocardial PG and GAG accumulation.[10-13] Following ischemia-reperfusion injury, CS accumulation inhibits sympathetic nerve re-innervation into the infarct area, leading to increased arrhythmogenicity.[14] Conversely, mice lacking the CS-rich proteoglycan (CSPG) receptor PTP-σ displayed reduced arrhythmia susceptibility.[15, 16] In the central nervous system, CS degradation *in vivo* mediated by the bacterial enzyme chondroitinase ABC (chABC),[17-19] or rhASB[20] critically promoted post-injury functional

Disclaimer: The manuscript and its contents are confidential, intended for journal review purposes only, and not to be further disclosed.

recovery. We therefore hypothesized a role for CS in non-MPS pathological cardiac remodeling, and tested the utility of CS targeting in heart failure (HF) treatment.

Methods

The data, analytic methods, and study materials will be/have been made available to other researchers for purposes of reproducing the results or replicating the procedure.[69]

Human LV tissue

Human left ventricular (LV) tissue was collected with a protocol approved by the Papworth Hospital (Cambridge) Tissue Bank Review Board and the Cambridgeshire Research Ethics Committee (UK). Written consent was obtained from every individual according to the Papworth Tissue Bank protocol. LV explants were from Caucasian male patients undergoing cardiac transplantation for end-stage cardiomyopathy (EsCM). Normal LVs were from healthy Caucasian age-matched male individuals (UK Human Tissue Bank, de Montfort University, UK). At the time of transplantation or donor harvest, whole hearts were removed after preservation and transported as previously described.[21] Individual sample details are listed in Supplementary Table 1.

Human and mouse primary cell culture and in vitro treatment

Human primary cardiac fibroblasts (CF) and coronary artery endothelial cells (EC) were purchased from PromoCell; coronary artery smooth muscle cells (SMC) were purchased from Thermo Scientific (donor information listed in Supplementary Table 2). Cells were cultured according to manufacturer's instructions. Macrophages were obtained by differentiating THP-1 cells with PMA treatment at 100 nM for 24 h. Mouse primary cardiomyocyte (CM) and CF were isolated as described before [22].

Hypoxia treatment was performed by subjecting cells to 0.2% oxygen for 2 or 24 h. Oxidative stress was applied by adding tert-butyl hydroperoxide (TBH) 50 μM (TBH 50) or 200 μM (TBH 200) into the human cardiac cell culture media for 4 h. TBH concentration used in mouse CM was 1 μM and 5 μM instead to account for higher sensitivity to toxicity. Cytokines including IL-1β, TGFβ, TNFα

Disclaimer: The manuscript and its contents are confidential, intended for journal review purposes only, and not to be further disclosed.

(Peprotech) and angiotensin II (Ang-II, Sigma) were added to the cell culture media at 10 ng / ml each for 4 h. The combined "HIT" treatment involved first subjecting cells to 24 h hypoxia, followed by adding IL-1β and TGFβ into culture media at 10 ng / ml each during the last 4 h.

For TNFα treatment experiments, CS-A was coated onto plastic substrate by incubating cell culture wells with 50 µg / ml CS-A solution for 2 h at 37 ºC. RhASB pretreated CS-A was prepared by adding 50 µg / ml CS-A and 50 µg / ml rhASB in Ca^{2+} + PBS, and incubating on wells for 2 h at 37 ºC. Excess incubating solution was removed by washing after 2 h. TNFα recombinant protein was then added to the wells and incubated for a further 20 min at 37ºC. Unbound TNFα was removed by washing with PBS thereafter. EC or macrophages were finally seeded onto the substrate and cultured for 6 h. Cells were harvested in TriReagent (Qiagen) for RNA extraction.

In vivo procedures

All animal procedures were performed according to a protocol approved by the National University of Singapore IACUC committee. Animal grouping was blinded to the main experimenters until data collection was finalized.

Pressure-overload was performed by applying an incompletely closed vessel occlusion clip (Weck Haemoclip) around the aorta between the branches of the brachiocephalic artery and the left carotid artery[23]. A fixed width of the occlusion clip was achieved by adjusting the closure to the width of a 0.5 mm metal wire. Transverse aortic Doppler ultrasound examination was performed for each rat to verify equal pressure gradients across the occlusion clip stenosis. 15 adult animals received sham surgery and 25 received TAC surgery. Four animals which received TAC surgery died within the first 24 h of surgery and were excluded from subsequent study analysis. Groups were assigned in random order. RhASB (BioMarin, Naglazyme, 1 mg / ml) or saline was injected at 1 ml / kg BW intravenously through the tail vein each week, and echocardiography was performed weekly. Rats were euthanized 10 weeks after TAC or sham surgery. For sham surgery, rats underwent thoracotomy but the occlusion clip was not applied. RhASB administration route, frequency and dosage were used

Disclaimer: The manuscript and its contents are confidential, intended for journal review purposes only, and not to be further disclosed.

as in clinical practice[24]. Sample size in each group were: sham+saline (S+S), N=12; sham+rhASB (S+A), N=3; TAC+saline (T+S), N=12; TAC+rhASB (T+A), N= 9. To study the temporal profile of C4S accumulation, TAC surgery was performed in six additional rats. These hearts were harvested on week 1, 2 and 4 post-TAC; N=2 per group.

For the isoprenaline model, isoprenaline (MedChem Express) was administered by osmotic mini-pump (2ML2, Alzet) over 4 weeks. Isoprenaline was diluted to 20 mg / ml in saline, and rats received on average 3 mg / kg bodyweight (BW) per day. By week 5, animals whose EF were still above 70% (N=6) were excluded from subsequent procedures. Control animals received sham surgery without pump implantation. Animals were randomized at week 5 to receive either rhASB (BioMarin, Naglazyme, 1 mg / ml) or saline at 1 ml / kg BW via the tail vein each week. Echocardiography was performed at fixed time points. Animals were euthanized 9 weeks after the start of isoprenaline treatment. Sample size in each group was: Sham+saline (S+S), N=8; Sham+rhASB (S+A), N=7; Isoprenaline+saline (I+S), N=9; Isoprenaline+rhASB (I+A), N=9.

Statistical analysis

Statistical analysis was performed in Graphpad Prism (GraphPad Software, Inc) with one-way ANOVA (for comparison between 4 groups) or Student's t-test (for comparison between two groups). Results are shown as mean ± SEM with specific tests used in each of the figures and tables provided in their corresponding legends. The sample size for animals, cells, or tissue samples in each group is also displayed in the legends of figures and tables.

See supplemental materials for further methods on LCMS, CS quantification assay, RT-qPCR (Supplementary Table 3 and 4 for gene and primer lists), histology methods (Supplementary Table 5 for antibody list), and surface plasmon resonance experiments.

Results

CS accumulation in failing human hearts

Disclaimer: The manuscript and its contents are confidential, intended for journal review purposes only, and not to be further disclosed.

First, we performed CS immunostaining with the monoclonal antibody 2H6, which probes for the major CS component of C4S, N-acetylgalactosamine-4-sulfate (Figure 1A, Supplementary Figure 1). Left ventricular (LV) sections were from non-MPS HF patients with end-stage cardiomyopathy (EsCM) and age-, gender- and race-matched healthy controls (N=6 each, sample details listed in Supplementary Table 1). In EsCM LV samples, there was consistent and significant perivascular and interstitial CS accumulation, particularly in regions of intense fibrosis (Figure 1A, Supplementary Figure 1). We further quantified total GAG content in extracted GAGs and CS using an Alcian blue assay. Total GAG in EsCM samples was three times more abundant than in healthy controls (Figure 1B; 3.43 ± 1.33 μg / mg dry weight of lyophilized heart tissue vs. 1.02 ± 0.37 μg / mg; p=0.003). In particular, CS was three-fold more abundant in EsCM (2.23 ± 1.06 μg / mg vs. 0.71 ± 0.29 μg / mg; p=0.009). We proceeded to sub-analyze CS disaccharide relative composition by liquid chromatography-mass spectrometry (LCMS). Similar to the CS composition in other organs,[25] C4S was indeed the main CS component in human LV (Figure 1C). Relative CS composition remained unchanged between control and EsCM LV samples (Figure 1C).

Cell-specific analysis for CSPG regulation

To gain a clearer insight into CS deregulation in the failing heart, we asked which myocardial cell types were responsible for CSPG accumulation, and which stimulants triggered the change. Since GAG synthesis, unlike nucleic acids or proteins, is not template driven but is instead dynamically modulated by a series of processing enzymes,[26] we profiled for the mRNA expression of genes encoding for GAG processing enzymes, as an indication of overall GAG synthesis and processing in the different cell types of the heart (Figure 2). This included mRNA expression of CSPG protein cores, GAG chain initiation and elongation enzymes, CS sulfatases, and CS degradation enzymes. In addition, since a large proportion of CSPGs are known to bind to HA,[27] we also profiled for HA synthases (see Supplementary Table 3 for the full gene list). We quantified the expression of these mRNAs in a panel of human primary myocardial cell types comprising of cardiac fibroblasts (CF), smooth muscle cells (SMC) and endothelial cells (EC). Since macrophage infiltration may be relevant to CSPG biology in the myocardium, we also included the monocyte cell line THP-1 and

Disclaimer: The manuscript and its contents are confidential, intended for journal review purposes only, and not to be further disclosed.

macrophages differentiated from THP-1 cells with phorbol myristate acetate (PMA) treatment. Notably, all 4 cell types were positive for C4S by immunostaining (Figure 3A). Cell identity was validated by morphology (Figure 3A), and expression of their respective cell-type specific markers (Supplementary Figure 2A). Each cell type was subjected to 9 different culture conditions (Figure 2).

Related to the expression of the CSPG protein-core, we found that the large HA-binding versican gene (*VCAN*) was highly expressed in CF and SMC, the small leucine-rich proteoglycans (SLRPs) decorin (*DCN*) and lumican (*LUM*) genes were expressed in CF, and biglycan (*BGN*) expression was detected in CF, SMC and EC. Low expression of the cell surface CSPG CD44 in monocytes and macrophages was upregulated following exposure to oxidative stress (tert-butyl hydroperoxide, TBH) and by IL-1β. *DCN*, but not *VCAN*, was upregulated in CF by 24 h hypoxia, whereas expression of all other protein-core genes was not altered by stimulation (Figure 2A). Related to CS chain synthesis, the gene for the GAG chain initiation enzyme xyloside transferase 1 (*XYLT1*) was highly upregulated by TGFβ in CF and SMC. The CS chain elongation enzyme *CHPF* was highly expressed in CF and SMC, and *CHSY1* was preferentially expressed in macrophages. *CHPF* was upregulated in CF by hypoxia and TBH-induced oxidative stress. *CHSY1* was upregulated in macrophages by all treatment conditions (Figure 2B). A further step in GAG synthesis is CS sulphation. The C4S sulfotransferase gene, *C4ST1*, was expressed in macrophages, and further significantly upregulated in CF by IL-1β, TNFα and TGFβ. In the other cell types, the main sulfotransferase expressed was the D4S sulfotransferase *D4ST1* (Figure 2C).

In the pathways leading to CS degradation, *ARSB* was expressed more in SMC than in other cell types. However, mRNA abundance for all GAG degradation enzymes was notably unaltered by any condition (Figure 2D). Western blot also showed no significant change in ASB protein induced by any treatment condition (Figure 3E), reflecting the overall likelihood that myocardial cell types do not effectively upregulate CS degradation to counterbalance the increased expression of genes related to CS synthesis. Despite being known as a lysosomal enzyme, we found that the ASB enzyme was

Disclaimer: This manuscript and its contents are confidential, intended for journal review purposes only, and not to be further disclosed.

abundant in CF conditioned media in addition to cell pellet lysates (Figure 3E), suggesting that at least in this context, ASB is secreted by CF in significant quantities.

CSPG production in CM was measured in CM and CF freshly isolated from mouse hearts due to the unavailability of primary human CM. Gene expression of PG core proteins and *C4ST1* under similar culture conditions as described above were measured with RT-qPCR (Supplementary Figure 2B, C). Compared to mouse CF (mCF), CSPG production was virtually absent in mouse CM (mCM). Cell viability and the mCM stress-response were confirmed by expression levels changes in *Nppb*.

Since CF convincingly integrated mRNA increases responsible for CSPG protein core synthesis (e.g. *DCN*), CS chain elongation (e.g. *CHSY1* and *CHPF*) and CS sulfation (*C4ST1*), and we had found significant CS accumulation in areas of myocardial fibrosis in our failing hearts, we chose CF to pursue a more detailed investigation into stress-induced CSPG upregulation. Consistent with the findings above, TGFβ upregulated the gene expression of CS chain initiation and elongation enzymes, and IL-1β upregulated the expression of C4S sulfotransferase in CF (Figure 3B). A C4S dot blot using conditioned media collected from CF treated with hypoxia, IL-1β or TGFβ alone, and the combination of all three ("HIT" treatment), confirmed that TGFβ induced C4S increase, further augmented by the "HIT" combination treatment (Figure 3C). We further investigated whether these treatment conditions also induced CS chain extension by using decorin (DCN) as a CSPG representative. DCN is a small CSPG with one GAG chain of either CS or DS. GAG chain length can thus be deduced by comparing the difference in molecular weight (MW) between the complete CSPG (i.e. DCN with GAG chain) and its protein core alone (DCN without CS chain). Empirically, the protein core can be obtained by treating CSPGs with chABC, a potent bacterial enzyme that digests all CS / DS GAG chains into disaccharides. We noted that the abundance of the DCN protein core was increased by hypoxia, TGFβ and combined "HIT" conditions (DCN without CS chain in Figure 3D). Concurrently, MW of complete DCN was increased from 75 kD to ~100 kD by the combined "HIT" treatment (DCN with CS chain in Figure 3D). Since MW of the DCN core protein is not expected to change, the MW increase of complete DCN may be attributed to increased CS chain extension, implying that at least

Disclaimer: The manuscript and its contents are confidential, intended for journal review purposes only, and not to be further disclosed.

for the example of DCN, treatment conditions upregulated CSPG abundance and also CS chain length extension.

High MW molecules secreted by CF activated IL1B upregulation in macrophages

Next, we noted that "HIT" treatment in CF also induced a two-fold increase in secreted proteins (Figure 3F). We collected the conditioned media, and filtered and concentrated it with a 50kD MW cut-off membrane. Cytokines with low MW (<20kD) were filtered away, leaving behind only high MW secreted proteins. When added to a macrophage culture, CF-secreted high MW proteins induced *IL1B*, but not *TNFA*, gene upregulation in macrophages differentiated from THP-1 cells (Figure 3G, H). The level of *IL1B* gene upregulation was comparable to that of direct macrophage stimulation with IL-1β and TGFβ at 10 nM / ml, suggesting that under pathological conditions, CFs secreted large extracellular molecules with inflammatory properties, capable of activating immune cells through specific pathways. Although this conditioned media is expected to contain a myriad of large extracellular molecules, many of which could possess pro-inflammatory properties, we have verified that "HIT" treatment induced a dramatic increase in secreted CSPGs containing C4S (Figure 3C).

CS accumulation in a rat model of pressure-overload cardiac remodeling

Among rodents, rats rather than mice are similar to human in terms of CS production.[28] To test the generality of CS accumulation as a process of pathological remodeling in cardiomyopathy *in vivo*, we therefore analyzed myocardial CS changes in 2 rat models of pathological remodeling. First, we surgically induced pressure-overload by transverse aortic constriction (TAC) using the clip-TAC technique[23] (Figure 4A). The degree of stenosis was controlled by a mechanical stopping device to ensure consistency (Supplementary Figure 3A, 3B). In this model, myocardial hypertrophy was accompanied by significant accumulation of C4S (Figure 4B), similar to our findings in human hearts. C4S deposition was observed as early as 1 week post-TAC, persisted throughout the course of observation and co-localized to fibrotic regions as visualized by concurrent Sirius red (SR) staining (Supplementary Figure 3C). As in diseased human myocardium, C4S was also observed to accumulate in the perivascular space and the myocardial interstitium (Supplementary Figure 3C,

Disclaimer: The manuscript and its contents are confidential, intended for journal review purposes only, and not to be further disclosed.

Figure 4B). Additional staining for polysaccharides was performed with Alcian blue (AB) at pH 0.5, which stains only sulfomucins, or with colloidal iron (CI), which stains total mucin. In the TAC heart, both staining patterns replicated that of the 2H6-antibody for C4S, and also co-localized well with regions of fibrosis (Figure 4C). Taken together, this provided good evidence that the sulfomucin CS is accumulated in fibrotic regions of the pathologically remodeled LV.

Systemic rhASB treatment in TAC rats reduced myocardial CS content

Complete CS degradation and turnover requires the removal of sulfate groups from sulfated disaccharides as part of the prerequisite sequential steps[28]. ASB is the sulfatase specific for C4S. Since C4S is the predominant component of myocardial CS in pathological remodeling (~80% of total CS, Figure 1C) and we had noted that under disease stimulus, cardiac cell types did not efficiently upregulate ASB abundance (Figure 3E), we proceeded to treat TAC-operated rats with rhASB to investigate its effect on cardiac CS and overall cardiac function (study design in Figure 4A). Immunofluorescence staining for C4S confirmed that rhASB treatment resulted in significant CS reduction (Figure 4C). We extracted and quantified CS from rat heart tissue by the end of rhASB treatment. Quantified with the Alcian blue assay, total CS abundance was increased by TAC ($p<0.001$) and significantly reduced by rhASB (Figure 4D, $p=0.022$). Relative CS disaccharide composition measured by LCMS showed a trend towards increased C0S proportion in the two rhASB treated groups (Figure 4E), whereas the disaccharide composition of another GAG group, HS, remained unchanged (Figure 4F).

RhASB treatment alleviated fibrosis, inhibited inflammation, and attenuated cardiac deterioration

Rats were divided into four groups to receive either sham surgery and saline or rhASB treatment (S+S; S+A), or TAC surgery and saline or rhASB treatment (T+S; T+A). TAC surgery induced significant hypertrophy, and a fall in ejection fraction (EF) compared to sham operated groups (Figure 5A, B). RhASB-treatment, initiated 2 weeks post-TAC, maintained EF during the treatment-course of 8-week post-TAC (Figure 5B; $p<0.001$). Posterior wall thickening (PWT), which measures the percentage change of posterior wall thickness between diastole and systole, and stroke volume (SV)

Disclaimer: The manuscript and its contents are confidential, intended for journal review purposes only, and not to be further disclosed.

showed sustained healthy myocardial function in the rhASB-treated group (Figure 5C-E), compared to saline treatment. Hypertrophy measured by histology, echocardiography, and heart weight/body weight ratio did not show significant changes in this experiment (Supplementary Figure 3D-G), possibly due to the constant presence of the surgical aortic constriction. Instead, myocardial fibrosis was significantly decreased by rhASB-treatment, compared to TAC and saline treatment (Figure 5F, G; 8.9 ± 0.67% and 5.9 ± 0.92% in T+S and T+A groups respectively; $p<0.001$).

Next, we searched for an underlying mechanism to explain the positive effects of rhASB. Fibrosis and immune responses in the cardiac ECM are closely linked processes, and we had found above that CF-secreted CSPGs may modify immune responses. We therefore quantified the immune reaction in our rat LV by counting the number of macrophages (Figure 5H, I), infiltrating CD45+ leukocytes and CD3+ T-cells (Supplementary Figure 4). Macrophages were visualized by immunostaining with CD68 and anti-Iba1 antibodies. CD68+ macrophage count was significantly increased in the TAC operated group compared to sham (Figure 5H, I; 68.08 ± 4.91 vs. 29.51 ± 4.05 cells / mm^2 in T+S and S+S groups, respectively), and significantly decreased by rhASB treatment (35.61 ± 5.97 cells / mm^2 in T+A group, $p<0.001$). We observed a similar result in Iba+ macrophages (Supplementary Figure 4E, F). CD45+ leukocytes displayed the same response, with a significant reduction by rhASB treatment (Supplementary Figure 4A, B; 42.08 ± 21.10 (S+S), 48.03 ± 13.21 (S+A), 89.60 ± 32.12 (T+S) and 55.11 ± 19.94 (T+A) cells / mm^2; $p<0.001$). In contrast, CD3+ T-cells were present in relatively low numbers at this chronic stage, with no significant differences among the different groups (Supplementary Figure 4C, D; 3.6 ± 3.08 (S+S), 5.1 ± 3.18 (S+A), 6.1 ± 3.91 (T+S) and 4.5 ± 2.63 (T+A) cells / mm^2).

RhASB rescued cardiac function in the isoprenaline-infusion model of pathological remodeling

In the next *in vivo* experiment, we tested the effect of delayed rhASB treatment in rats implanted with subcutaneous osmotic pumps releasing isoprenaline at an average rate of 3 mg / kg BW for 4 weeks. Isoprenaline induces cardiomyocyte necrosis through activating the β-adrenergic pathway.[29] Two weeks post commencement of isoprenaline infusion, we observed regions of severe ischemic injury,

Disclaimer: The manuscript and its contents are confidential, intended for journal review purposes only, and not to be further disclosed.

co-localized with abundant CD45+ leukocyte infiltrate (Supplementary Figure 5A, B). By week 5, EF in the isoprenaline-treated rats was reduced to 62.55 ± 6.4%. Five weekly rhASB injections were initiated from week 5 after isoprenaline infusion (Figure 6A).

First, we compared the CS and HS distribution patterns again in the rat heart sections after two weeks of isoprenaline treatment. Overall polysaccharide staining with colloidal iron and acidic sulfated polysaccharide with Alcian blue (AB) at pH 0.5 indicated enrichment of polysaccharides, especially acidic sulfated polysaccharides in the fibrotic regions. Specific immunostaining with monoclonal antibodies for CS (CS56), C4S (2H6) and HS (10E4) revealed that CS, especially C4S, was highly enriched in the fibrotic regions (Figure 6B, C), whereas HS distribution was more homogenous (Supplementary Figure 5C, D). This effectively recapitulates the consistent pattern of C4S, but not HS, accumulation again in fibrotic regions of pathological cardiac remodeling.

By week 9, we observed a reduction of fibrosis in rhASB treated animals, compared to saline treated animals; accompanied by a decreased level of sulfated polysaccharides (observed by AB staining at pH 0.5), and C4S content (2H6, Figure 6B). Myocardial fibrosis was again significantly lower with rhASB-treatment (Figure 6D, SR staining; 3.2 ± 0.56%, 3.0 ± 0.85%, 9.9 ± 2.67% and 6.61 ± 1.66% fibrotic area in S+S, S+A, I+S, I+A groups respectively). Echocardiography displayed a significantly accelerated recovery of contractile functional in the rhASB treated group (Figure 7A-C). Remarkably, some rhASB-treated animals recovered to the normal functional range as assessed by their EF (Figure 7D). Similar recovery was seen with PWT and SV (Figure 7E, F).

TNFα bound directly to CS GAG and mediated downstream gene expression responses

CSPGs are known triggers of inflammation by activating toll-like receptors.[30-34] Hence, we investigated if myocardial CSs, like other GAGs, mediated their effect by presenting specific extracellular ligands to cell surfaces, thereby activating cellular downstream signaling. We first assayed for the disaccharide composition of commercial biotinylated CS products by LCMS, and found that the CS-A product has a similar composition to human and rat heart CS (Figure 8A). Then,

Disclaimer: The manuscript and its contents are confidential, intended for journal review purposes only, and not to be further disclosed.

in order to identify ligands of CS in myocardial ECM, we undertook a candidate approach and performed CS-protein interaction assays using the Surface Plasmon Resonance (SPR) system.

Biotinylated CS, CS-A, heparin or BSA was pre-bound to the ProteOn NeutrAvidin-coated NLC sensor chip, and the affinity between GAGs and candidate proteins was measured. Heparin was used as a positive control as it has the highest negative charge of all GAGs, and was hence expected to display the strongest protein-binding affinity (Figure 8B). Bovine serum albumin (BSA) was used as the reference to which each interaction was normalized. As anticipated, CS had a very low binding affinity to human serum albumin (HSA), fibrinogen and IgG (Figure 8B), corresponding to its overall anti-protein adhesion function. Among the candidate cytokines, TNFα, but not TGFβ or IL-6, bound strongly to CS-A, suggesting a unique and specific affinity between TNFα and CS-A. In particular, the interaction between CS-A and TNFα was not dissociated by high-salt buffer or detergent washing.

Lastly, we undertook *in vitro* experiments to assess the direct effect of CS-A and TNFα binding. Cell culture plates were pre-coated with poly-D-lysine (PDL), CS-A, or CS-A and rhASB, and subsequently pre-incubated with TNFα, before washing of plates, and seeding of primary human CFs. Expression of the TNFα target gene *VCAM1* was assessed. TNFα bound to CS-A, but not PDL, and effectively upregulated *VCAM1* expression (Figure 8C), confirming that the binding effect of CS-A indeed supports TNFα signalling activation, rather than sequestering or decoying TNFα. The same effect was also observed when performing the experiment on macrophages differentiated from THP-1 cells. Macrophage activation was measured by qPCR of the *TNFA* gene (Figure 8D). Remarkably, *TNFA* signal activation was completely abolished when cells were cultured on CS-A which was pre-treated with rhASB, reflecting the potent negative effect of rhASB on CS-A-mediated TNFα downstream signaling.

Discussion

Proteoglycan complexes are widely synthesized in connective tissue, platelets and blood vessels[35]. In cardiac disease, HSPGs and HA have been extensively studied in the context of vascular disease and

Disclaimer: The manuscript and its contents are confidential. Intended for journal review purposes only, and not to be further disclosed.

myocardial fibrosis, immune cell recruitment, ECM remodeling and cardiac dysfunction.[36-43] On the other hand, much less is known about the role of CSPGs and CS GAG in cardiac remodeling. CSPGs are molecules consisting of protein cores and CS GAG chains. Differentially attached CS chains may modify the functional behavior of CSPGs.[30, 32, 33] In this study, we have comprehensively investigated the composition, synthesis, regulation and mechanistic interactions of myocardial CS, and uncovered its remarkable potential for targeting cardiac fibrosis in pathological remodeling.

Although patients with other forms of MPS also show multi-organ GAG accumulation, including in the myocardium, our discovery of the predominant C4S component in non-MPS failing hearts led us to focus on the more generic relevance of MPS VI. Patients with the monogenic disease MPS VI harbor loss-of-function mutations in the *ARSB* gene and indeed manifest a range of systemic conditions, including heart failure, reflecting the importance of CS regulation in maintaining normal cardiac function. Characterization of total myocardial CS by LCMS revealed that the relative disaccharide composition remained constant between health and disease, and C4S was the predominant CS component. This observation was replicated in two rat models of pathological cardiac remodeling.

In vitro screening for CSPG-related genes showed that different cardiac cell types employed different enzymes for differential CS synthesis. Interestingly, macrophages exclusively expressed the C4S sulfotransferase *C4ST1*, whereas the D4S sulfotransferase *D4ST1* was highly expressed in other cell types. C4S and D4S are stereo-isomers. This raises the possibility that the CS / DS molecular chirality plays a role in mediating their molecular interactions in the myocardium. Nonetheless, for CSPG regulation, we found that TGFβ was sufficient to induce CS upregulation, and the combination of hypoxia, IL-1β and TGFβ ("HIT") not only upregulated CSPG abundance, but also CS chain extension, as represented by the increase in overall Decorin molecular weight. Since *in vivo* pathophysiology involves the combined effect of hypoxia and cytokines, this result is consistent with the notion that CSPGs are indeed upregulated both in abundance and in chain length in diseased hearts.

Disclaimer: The manuscript and its contents are confidential, intended for journal review purposes only, and not to be further discussed.

In human primary cardiac fibroblast culture, we found that ASB is abundantly secreted into the media, despite being classically known as a lysosomal enzyme. Weekly infusion of rhASB is the FDA-approved treatment for MPS VI patients, targeted to reduce systemic GAG accumulation.[6, 24, 44] In a rodent model of spinal cord injury, rhASB effectively eliminated CS using a single injection into spinal cord tissue, leading to increased axon regeneration and improved motor function[20]. In human endothelial cells, rhASB negatively regulated CSPG versican expression and reduced versican-attached C4S.[45] ASB repression reproduced the effect of hypoxia with increased C4S content, while ASB overexpression reduced nuclear HIF level.[46] In this study we observed that systemic rhASB treatment effectively reduced total myocardial CS content in the rat models of HF. Early rhASB treatment prevented TAC-induced functional deterioration in the TAC model without affecting cardiac hypertrophy. In human MPS VI patients, rhASB significantly improved hypertrophy in patients younger, but not those older, than 12 years old. Interestingly, this difference may be because in older patients, chronic GAG deposition had caused irreversible aortic valve deformation resulting in fixed aortic stenosis. Hypertrophy was therefore unchanged in the presence of the fixed unaltered pressure gradient[8]. In our TAC model the lack of hypertrophic improvement may also be explained in a similar way since the TAC pressure gradient was also not removed. Nonetheless, cardiac functional improvement, despite unchanged hypertrophy, suggests that fibrosis reduction resulted from an inhibition of pathological processes that also influence contractility. We speculate that this is likely due to positive myocardial remodeling itself since the extracellular matrix, including inflammatory infiltrates, was significantly different in ASB-treated animals. To circumvent the issue of sustained pressure gradient in the TAC model, we turned to the isoprenaline-infusion model to test for fibrosis rescue. Here, after the onset of pathology with isoprenaline-infusion, we were still able to find improved fibrosis and functional rescue from delayed rhASB treatment, consistent indeed to a property of fibrosis rescue.

As a large class of GAG molecules, CSPGs comprise of multiple forms with many overlapping functions, including small collagen binding proteins with inflammatory properties (e.g. SLRPs

Disclaimer: The manuscript and its contents are confidential, intended for journal review purposes only, and not to be further discussed.

decorin and biglycan), large HA-binding ECM proteins (e.g. versican) and membrane proteins (e.g. CD44). The effect of CSPG modifications in the heart are therefore likely to be complex and multi-faceted, and probably involve multiple cell types including immune cells, vascular cells, cardiac nerves, and others. Here we focused our investigation on one potential mode of action. Fibrosis and chronic inflammation in the heart are known to perturb contractile function, [47-52] and inflammatory processes are major mediators of cardiac fibrosis.[53-57] In rats, rhASB treatment led to reduced numbers of CD45-positive immune cells, as well as CD68 and Iba-1-positive macrophages, supporting a functional role for CS in aggravating the myocardial inflammatory cell response during pathological remodeling. CSPGs are mediators of both innate and adaptive immune responses.[58] While under normal conditions CSPGs are membrane- or ECM-bound, and do not trigger an immune reaction, soluble CSPGs derived from proteolytic digestion of ECM or CSPGs newly synthesized by macrophages are recognized as potent danger signals.[59] CSPGs versican and decorin activate macrophages and other myeloid cells to secrete pro-inflammatory cytokines through binding to toll-like receptors (TLRs), CD44 and mannose receptors.[32, 60-62] The GAG component is indispensable for the interaction with cell surface receptors and consequent immune cell activation.[31, 59, 63] Our work now sheds light on how CSPG accumulation in pathological cardiac remodeling integrates signals contributing to the inflammation and fibrotic processes. Furthermore, we identified TNFα as a direct binding partner to CS GAG chains. Notably, the binding to TNFα did not require the presence of the PG protein core. TNFα bound to CS-A triggered upregulation of genes in the TNFα pathway in EC and macrophages, which was in turn, significantly inhibited by rhASB. This is consistent with the model that CS-A GAGs present TNFα to cells, rather than sequester or decoy the molecule, and that the *in vivo* rhASB effect is at least partly due to the interference of the TNFα pathway. Remarkably, this finding is also consistent with data from early clinical studies where an increased TNFα mRNA level was observed in MPS VI patients compared to healthy controls, and was reduced by five-fold after one month of rhASB treatment.[64, 65] All together, these lines of evidence suggest that CSPGs induce inflammation through interaction between the CS GAG chain and TNFα, in addition to direct activation of immune cells through their cell surface receptors.

Disclaimer: This manuscript and its contents are confidential, intended for journal review purposes only, and not to be further disclosed.

Finally, CSPGs decorin and biglycan belong to the category of SLRPs that bind to collagen and facilitate collagen fibril formation and fiber alignment.[66, 67] Decorin and biglycan double deficient mice displayed reduced collagen synthesis.[68] It is conceivable that interfering with collagen-binding CSPGs also affects collagen fiber formation or stability, thereby reducing collagen synthesis or increasing collagen turnover. Further studies will be necessary to investigate whether collagen organization and stability is altered by rhASB treatment.

Taken together, our results indicate for the first time that myocardial CSPG accumulation is maladaptive and triggers inflammatory and pro-fibrotic processes in pathological cardiac remodeling. GAG regulation is delicately controlled by environmental cues through the regulation of a battery of GAG synthesis and degradation enzymes, and played out by the different important myocardial cell types. Targeting CS accumulation such as with rhASB represents a novel therapeutic approach for pathological cardiac remodeling in HF.

Disclaimer: The manuscript and its contents are confidential, intended for journal review purposes only, and not to be further disclosed.

Acknowledgments

We thank Dr. Raymond Alexander Alfred Smith, Dr. Chaw Su Yin, Dr. Wang Tian Hua, Ellen Tejo and Dr. Luu Danh Anh Tuan for sharing expertise and for their generous help with the experiments.

Source of Funding

This work was supported by Singapore Agency for Science, Technology and Research (A*STaR) Biomedical Research Council (BMRC) and Singapore National Medical Research Council (NMRC) grants.

Declaration of conflict of interest

None

References

1. Brown L. Cardiac extracellular matrix: a dynamic entity. *Am J Physiol Heart Circ Physiol*. 2005;289:H973-4.
2. Rienks M, Papageorgiou AP, Frangogiannis NG and Heymans S. Myocardial extracellular matrix: an ever-changing and diverse entity. *Circ Res*. 2014;114:872-88.
3. Arroyo AG and Iruela-Arispe ML. Extracellular matrix, inflammation, and the angiogenic response. *Cardiovasc Res*. 2010;86:226-35.
4. Miner EC and Miller WL. A look between the cardiomyocytes: the extracellular matrix in heart failure. *Mayo Clin Proc*. 2006;81:71-6.
5. Travers JG, Kamal FA, Robbins J, Yutzey KE and Blaxall BC. Cardiac Fibrosis: The Fibroblast Awakens. *Circ Res*. 2016;118:1021-40.
6. Braunlin EA, Harmatz PR, Scarpa M, Furlanetto B, Kampmann C, Loehr JP, Ponder KP, Roberts WC, Rosenfeld HM and Giugliani R. Cardiac disease in patients with mucopolysaccharidosis: presentation, diagnosis and management. *J Inherit Metab Dis*. 2011;34:1183-97.
7. Oudit GY, Butany J, Williams WG, Clarke JT and Iwanochko RM. Images in cardiovascular medicine. Left ventricular aneurysm associated with mucopolysaccharidosis type VI syndrome (Maroteaux-Lamy syndrome). *Circulation*. 2007;115:e60-2.
8. Braunlin E, Rosenfeld H, Kampmann C, Johnson J, Beck M, Giugliani R, Guffon N, Ketteridge D, Sa Miranda CM, Scarpa M, Schwartz IV, Leao Teles E, Wraith JE, Barrios P, Dias da Silva E, Kurio G, Richardson M, Gildengorin G, Hopwood JJ, Imperiale M, Schatz A, Decker C, Harmatz P and Group MVS. Enzyme replacement therapy for mucopolysaccharidosis VI: long-term cardiac effects of galsulfase (Naglazyme(R)) therapy. *J Inherit Metab Dis*. 2013;36:385-94.
9. McGill JJ, Inwood AC, Coman DJ, Lipke ML, de Lore D, Swiedler SJ and Hopwood JJ. Enzyme replacement therapy for mucopolysaccharidosis VI from 8 weeks of age--a sibling control study. *Clin Genet*. 2010;77:492-8.
10. Drobnik J, Szczepanowska A and Dabrowski R. Temporary augmentation of glycosaminoglycans content in the heart after left coronary artery ligation. *Pathophysiology*. 2004;11:35-39.
11. Huynh MB, Morin C, Carpentier G, Garcia-Filipe S, Talhas-Perret S, Barbier-Chassefiere V, van Kuppevelt TH, Martelly I, Albanese P and Papy-Garcia D. Age-related changes in rat myocardium involve altered capacities of glycosaminoglycans to potentiate growth factor functions and heparan sulfate-altered sulfation. *J Biol Chem*. 2012;287:11363-73.
12. Prante C, Milting H, Kassner A, Farr M, Ambrosius M, Schon S, Seidler DG, Banayosy AE, Korfer R, Kuhn J, Kleesiek K and Gotting C. Transforming growth factor beta1-regulated xylosyltransferase I activity in human cardiac fibroblasts and its impact for myocardial remodeling. *J Biol Chem*. 2007;282:26441-9.
13. Shetlar MR, Davitt WF, Rosett RL, Crass MF, 3rd, Lautsch EV and Kischer C. Glycosaminoglycan changes in healing myocardial infarction. *Proc Soc Exp Biol Med*. 1978;158:210-4.
14. Gardner RT and Habecker BA. Infarct-derived chondroitin sulfate proteoglycans prevent sympathetic reinnervation after cardiac ischemia-reperfusion injury. *J Neurosci*. 2013;33:7175-83.
15. Gardner RT, Ripplinger CM, Myles RC and Habecker BA. Molecular Mechanisms of Sympathetic Remodeling and Arrhythmias. *Circ Arrhythm Electrophysiol*. 2016;9:e001359.
16. Gardner RT, Wang L, Lang BT, Cregg JM, Dunbar CL, Woodward WR, Silver J, Ripplinger CM and Habecker BA. Targeting protein tyrosine phosphatase sigma after myocardial infarction restores cardiac sympathetic innervation and prevents arrhythmias. *Nat Commun*. 2015;6:6235.
17. Kwok JC, Heller JP, Zhao RR and Fawcett JW. Targeting inhibitory chondroitin sulphate proteoglycans to promote plasticity after injury. *Methods Mol Biol*. 2014;1162:127-38.
18. Zhao RR and Fawcett JW. Combination treatment with chondroitinase ABC in spinal cord injury--breaking the barrier. *Neurosci Bull*. 2013;29:477-83.
19. Zhao RR, Muir EM, Alves JN, Rickman H, Allan AY, Kwok JC, Roet KC, Verhaagen J, Schneider BL, Bensadoun JC, Ahmed SG, Yanez-Munoz RJ, Keynes RJ, Fawcett JW and Rogers JH. Lentiviral vectors express chondroitinase ABC in cortical projections and promote sprouting of injured corticospinal axons. *J Neurosci Methods*. 2011;201:228-38.

20. Yoo M, Khaled M, Gibbs KM, Kim J, Kowalewski B, Dierks T and Schachner M. Arylsulfatase B improves locomotor function after mouse spinal cord injury. *PLoS One*. 2013;8:e57415.
21. Choy MK, Movassagh M, Siggens L, Vujic A, Goddard M, Sanchez A, Perkins N, Figg N, Bennett M, Carroll J and Foo R. High-throughput sequencing identifies STAT3 as the DNA-associated factor for p53-NF-kappaB-complex-dependent gene expression in human heart failure. *Genome Med*. 2010;2:37.
22. Ackers-Johnson M, Li PY, Holmes AP, O'Brien SM, Pavlovic D and Foo RS. A Simplified, Langendorff-Free Method for Concomitant Isolation of Viable Cardiac Myocytes and Nonmyocytes From the Adult Mouse Heart. *Circ Res*. 2016;119:909-20.
23. Zaha V, Grohmann J, Gobel H, Geibel A, Beyersdorf F and Doenst T. Experimental model for heart failure in rats--induction and diagnosis. *Thorac Cardiovasc Surg*. 2003;51:211-5.
24. Braunlin E, Orchard PJ, Whitley CB, Schroeder L, Reed RC and Manivel JC. Unexpected coronary artery findings in mucopolysaccharidosis. Report of four cases and literature review. *Cardiovasc Pathol*. 2014;23:145-51.
25. Vallen MJ, Schmidt S, Oosterhof A, Bulten J, Massuger LF and van Kuppevelt TH. Primary ovarian carcinomas and abdominal metastasis contain 4,6-disulfated chondroitin sulfate rich regions, which provide adhesive properties to tumour cells. *PLoS One*. 2014;9:e111806.
26. Mikami T and Kitagawa H. Biosynthesis and function of chondroitin sulfate. *Biochim Biophys Acta*. 2013;1830:4719-33.
27. Johansson S, Hedman K, Kjellen L, Christner J, Vaheri A and Hook M. Structure and interactions of proteoglycans in the extracellular matrix produced by cultured human fibroblasts. *Biochem J*. 1985;232:161-8.
28. Kresse H and Glossl J. Glycosaminoglycan degradation. *Adv Enzymol Relat Areas Mol Biol*. 1987;60:217-311.
29. Teerlink JR, Pfeffer JM and Pfeffer MA. Progressive ventricular remodeling in response to diffuse isoproterenol-induced myocardial necrosis in rats. *Circ Res*. 1994;75:105-13.
30. Babelova A, Moreth K, Tsalastra-Greul W, Zeng-Brouwers J, Eickelberg O, Young MF, Bruckner P, Pfeilschifter J, Schaefer RM, Grone HJ and Schaefer L. Biglycan, a danger signal that activates the NLRP3 inflammasome via toll-like and P2X receptors. *J Biol Chem*. 2009;284:24035-48.
31. Kim S, Takahashi H, Lin WW, Descargues P, Grivennikov S, Kim Y, Luo JL and Karin M. Carcinoma-produced factors activate myeloid cells through TLR2 to stimulate metastasis. *Nature*. 2009;457:102-6.
32. Merline R, Moreth K, Beckmann J, Nastase MV, Zeng-Brouwers J, Tralhao JG, Lemarchand P, Pfeilschifter J, Schaefer RM, Iozzo RV and Schaefer L. Signaling by the matrix proteoglycan decorin controls inflammation and cancer through PDCD4 and MicroRNA-21. *Sci Signal*. 2011;4:ra75.
33. Schaefer L, Babelova A, Kiss E, Hausser HJ, Baliova M, Krzyzankova M, Marsche G, Young MF, Mihalik D, Gotte M, Malle E, Schaefer RM and Grone HJ. The matrix component biglycan is proinflammatory and signals through Toll-like receptors 4 and 2 in macrophages. *J Clin Invest*. 2005;115:2223-33.
34. Song R, Zeng Q, Ao L, Yu JA, Cleveland JC, Zhao KS, Fullerton DA and Meng X. Biglycan induces the expression of osteogenic factors in human aortic valve interstitial cells via Toll-like receptor-2. *Arterioscler Thromb Vasc Biol*. 2012;32:2711-20.
35. Wight TN and Merrilees MJ. Proteoglycans in atherosclerosis and restenosis: key roles for versican. *Circ Res*. 2004;94:1158-67.
36. Gonzales JC, Gordts PL, Foley EM and Esko JD. Apolipoproteins E and AV mediate lipoprotein clearance by hepatic proteoglycans. *J Clin Invest*. 2013;123:2742-51.
37. Gordts PL and Esko JD. Heparan sulfate proteoglycans fine-tune macrophage inflammation via IFN-beta. *Cytokine*. 2015;72:118-9.
38. Jiang D, Liang J, Campanella GS, Guo R, Yu S, Xie T, Liu N, Jung Y, Homer R, Meltzer EB, Li Y, Tager AM, Goetinck PF, Luster AD and Noble PW. Inhibition of pulmonary fibrosis in mice by CXCL10 requires glycosaminoglycan binding and syndecan-4. *J Clin Invest*. 2010;120:2049-57.
39. Liang J, Jiang D and Noble PW. Hyaluronan as a therapeutic target in human diseases. *Adv Drug Deliv Rev*. 2016;97:186-203.

40. Osterholm C, Folkersen L, Lengquist M, Ponten F, Renne T, Li J and Hedin U. Increased expression of heparanase in symptomatic carotid atherosclerosis. *Atherosclerosis*. 2013;226:67-73.
41. Vlodavsky I, Blich M, Li JP, Sanderson RD and Ilan N. Involvement of heparanase in atherosclerosis and other vessel wall pathologies. *Matrix Biol*. 2013;32:241-51.
42. Strand ME, Aronsen JM, Braathen B, Sjaastad I, Kvaloy H, Tonnessen T, Christensen G and Lunde IG. Shedding of syndecan-4 promotes immune cell recruitment and mitigates cardiac dysfunction after lipopolysaccharide challenge in mice. *J Mol Cell Cardiol*. 2015;88:133-44.
43. Strand ME, Herum KM, Rana ZA, Skrbic B, Askevold ET, Dahl CP, Vistnes M, Hasic A, Kvaloy H, Sjaastad I, Carlson CR, Tonnessen T, Gullestad L, Christensen G and Lunde IG. Innate immune signaling induces expression and shedding of the heparan sulfate proteoglycan syndecan-4 in cardiac fibroblasts and myocytes, affecting inflammation in the pressure-overloaded heart. *FEBS J*. 2013;280:2228-47.
44. Braunlin E, Mackey-Bojack S, Panoskaltsis-Mortari A, Berry JM, McElmurry RT, Riddle M, Sun LY, Clarke LA, Tolar J and Blazar BR. Cardiac functional and histopathologic findings in humans and mice with mucopolysaccharidosis type I: implications for assessment of therapeutic interventions in hurler syndrome. *Pediatr Res*. 2006;59:27-32.
45. Bhattacharyya S, Feferman L and Tobacman JK. Arylsulfatase B regulates versican expression by galectin-3 and AP-1 mediated transcriptional effects. *Oncogene*. 2014;33:5467-76.
46. Bhattacharyya S and Tobacman JK. Hypoxia reduces arylsulfatase B activity and silencing arylsulfatase B replicates and mediates the effects of hypoxia. *PLoS One*. 2012;7:e33250.
47. Cleutjens JP, Verluyten MJ, Smiths JF and Daemen MJ. Collagen remodeling after myocardial infarction in the rat heart. *Am J Pathol*. 1995;147:325-38.
48. Cohn JN, Ferrari R and Sharpe N. Cardiac remodeling--concepts and clinical implications: a consensus paper from an international forum on cardiac remodeling. Behalf of an International Forum on Cardiac Remodeling. *J Am Coll Cardiol*. 2000;35:569-82.
49. Gourdie RG, Dimmeler S and Kohl P. Novel therapeutic strategies targeting fibroblasts and fibrosis in heart disease. *Nat Rev Drug Discov*. 2016;15:620-38.
50. Jugdutt BI. Ventricular remodeling after infarction and the extracellular collagen matrix: when is enough enough? *Circulation*. 2003;108:1395-403.
51. van den Borne SW, Diez J, Blankesteijn WM, Verjans J, Hofstra L and Narula J. Myocardial remodeling after infarction: the role of myofibroblasts. *Nat Rev Cardiol*. 2010;7:30-7.
52. Weber KT. Cardiac interstitium in health and disease: the fibrillar collagen network. *J Am Coll Cardiol*. 1989;13:1637-52.
53. Dick SA and Epelman S. Chronic Heart Failure and Inflammation: What Do We Really Know? *Circ Res*. 2016;119:159-76.
54. Falkenham A, de Antueno R, Rosin N, Betsch D, Lee TD, Duncan R and Legare JF. Nonclassical resident macrophages are important determinants in the development of myocardial fibrosis. *Am J Pathol*. 2015;185:927-42.
55. Kawaguchi M, Takahashi M, Hata T, Kashima Y, Usui F, Morimoto H, Izawa A, Takahashi Y, Masumoto J, Koyama J, Hongo M, Noda T, Nakayama J, Sagara J, Taniguchi S and Ikeda U. Inflammasome activation of cardiac fibroblasts is essential for myocardial ischemia/reperfusion injury. *Circulation*. 2011;123:594-604.
56. Nicoletti A and Michel JB. Cardiac fibrosis and inflammation: interaction with hemodynamic and hormonal factors. *Cardiovasc Res*. 1999;41:532-43.
57. Van Linthout S, Miteva K and Tschope C. Crosstalk between fibroblasts and inflammatory cells. *Cardiovasc Res*. 2014;102:258-69.
58. Kolset SO, Prydz K and Pejler G. Intracellular proteoglycans. *Biochem J*. 2004;379:217-27.
59. Frey H, Schroeder N, Manon-Jensen T, Iozzo RV and Schaefer L. Biological interplay between proteoglycans and their innate immune receptors in inflammation. *FEBS J*. 2013;280:2165-79.
60. Buraschi S, Neill T, Goyal A, Poluzzi C, Smythies J, Owens RT, Schaefer L, Torres A and Iozzo RV. Decorin causes autophagy in endothelial cells via Peg3. *Proc Natl Acad Sci U S A*. 2013;110:E2582-91.
61. Wight TN. Versican: a versatile extracellular matrix proteoglycan in cell biology. *Curr Opin Cell Biol*. 2002;14:617-23.

62. Wu YJ, La Pierre DP, Wu J, Yee AJ and Yang BB. The interaction of versican with its binding partners. *Cell Res*. 2005;15:483-94.
63. Middleton J, Patterson AM, Gardner L, Schmutz C and Ashton BA. Leukocyte extravasation: chemokine transport and presentation by the endothelium. *Blood*. 2002;100:3853-60.
64. Di Natale P, Villani GR, Parini R, Scarpa M, Parenti G, Pontarelli G, Grosso M, Sersale G, Tomanin R, Sibilio M, Barone R and Fiumara A. Molecular markers for the follow-up of enzyme-replacement therapy in mucopolysaccharidosis type VI disease. *Biotechnol Appl Biochem*. 2008;49:219-23.
65. Polgreen LE, Vehe RK, Rudser K, Kunin-Batson A, Utz JJ, Dickson P, Shapiro E and Whitley CB. Elevated TNF-alpha is associated with pain and physical disability in mucopolysaccharidosis types I, II, and VI. *Mol Genet Metab*. 2016;117:427-30.
66. Chen S and Birk DE. The regulatory roles of small leucine-rich proteoglycans in extracellular matrix assembly. *FEBS J*. 2013;280:2120-37.
67. Kalamajski S and Oldberg A. The role of small leucine-rich proteoglycans in collagen fibrillogenesis. *Matrix Biol*. 2010;29:248-53.
68. Young MF, Bi Y, Ameye L and Chen XD. Biglycan knockout mice: new models for musculoskeletal diseases. *Glycoconj J*. 2002;19:257-62.
69. Materials will be made available through direct contact with the authors of this manuscript.

Disclaimer: The manuscript and its contents are confidential, intended for journal review purposes only, and not to be further disclosed

FIGURES

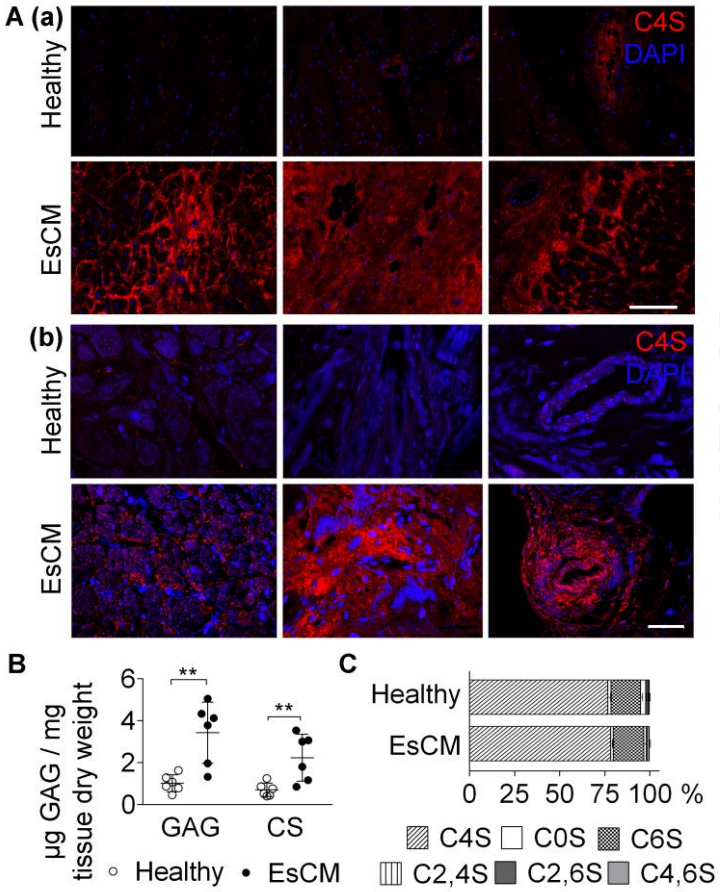

Figure 1. CS accumulation in left ventricles (LV) of human end-stage cardiomyopathic (EsCM) heart. (A) Immunostaining of C4S in healthy and EsCM LV sections. CS accumulation in EsCM was found in the interstitial space (left column), fibrotic regions (middle column), and perivascular space (right column). (a) Epifluorescent images. Scale bar, 100 µm. (b) Confocal images. Scale bar, 30 µm. See Supplementary Figure 1 for additional LV samples. **(B)** Quantification of extracted total GAG and CS with Alcian blue assay. GAG, $^{**}p=0.003$; CS, $^{**}p=0.009$ (Student's t-test). **(C)** CS disaccharide relative composition analysis by LCMS. C4S was the major CS component in both healthy and EsCM hearts. Relative composition of disaccharide subunits remained unchanged.

Disclaimer: The ... confidential, intended ... only, and not to ... s are ... urposes ... sed.

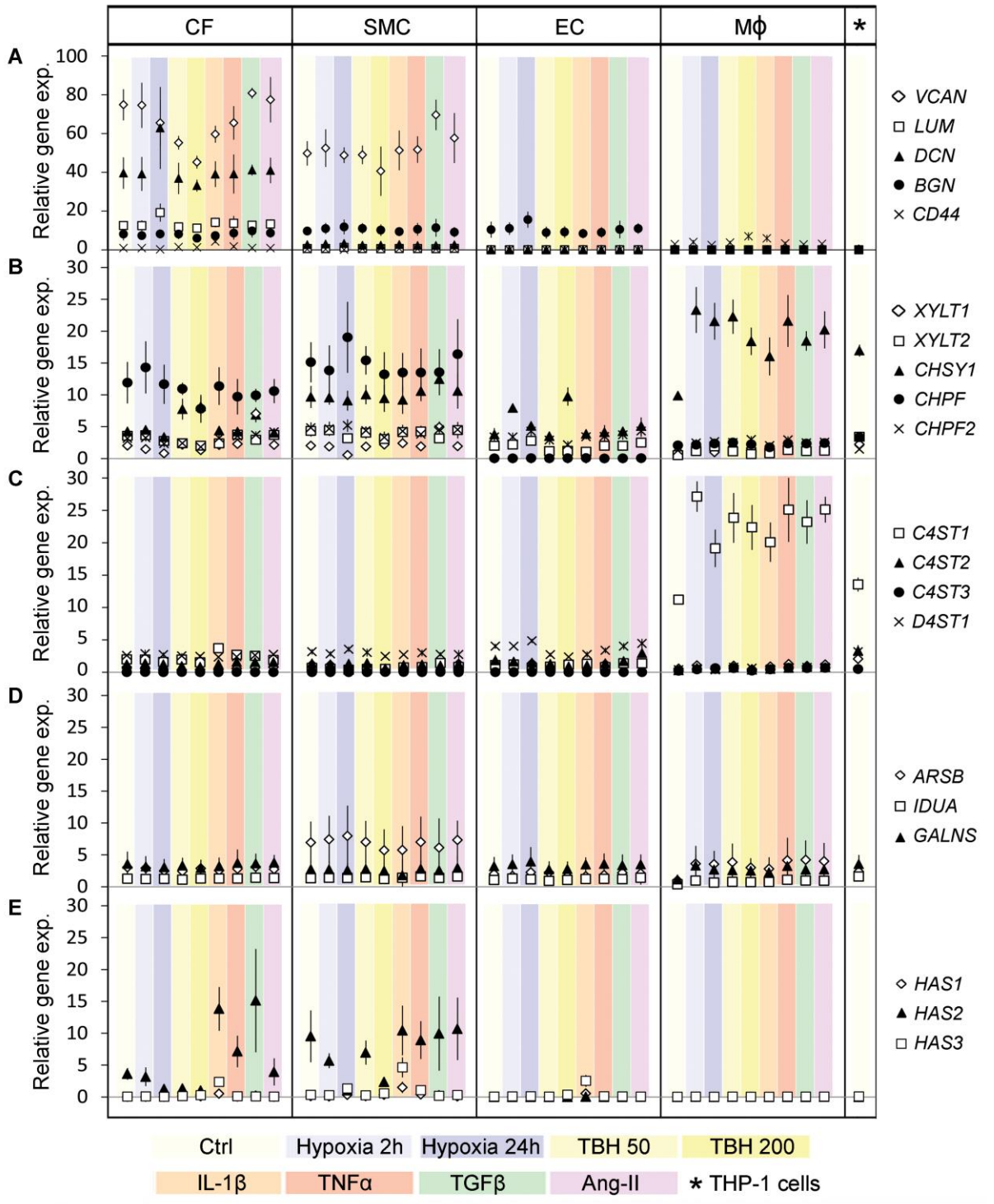

Figure 2. Expression profile of CSPG-related genes in primary human cardiac cells and THP-1 derived macrophages (Mφ) under different culture conditions. Expression of genes related to **(A)** CSPG protein cores, **(B)** enzymes for GAG chain initiation and CS chain elongation, **(C)** C4S / D4S sulfotransferases, **(D)** enzymes involved in CS / DS degradation, and **(E)** HA synthases. Each cell type was exposed to 9 culture conditions, represented by the different colour-coded background. Data

represent relative expression of each gene normalised to 10000th of 18S rRNA expression, presented as mean ± SD. N=3 for each culture condition.

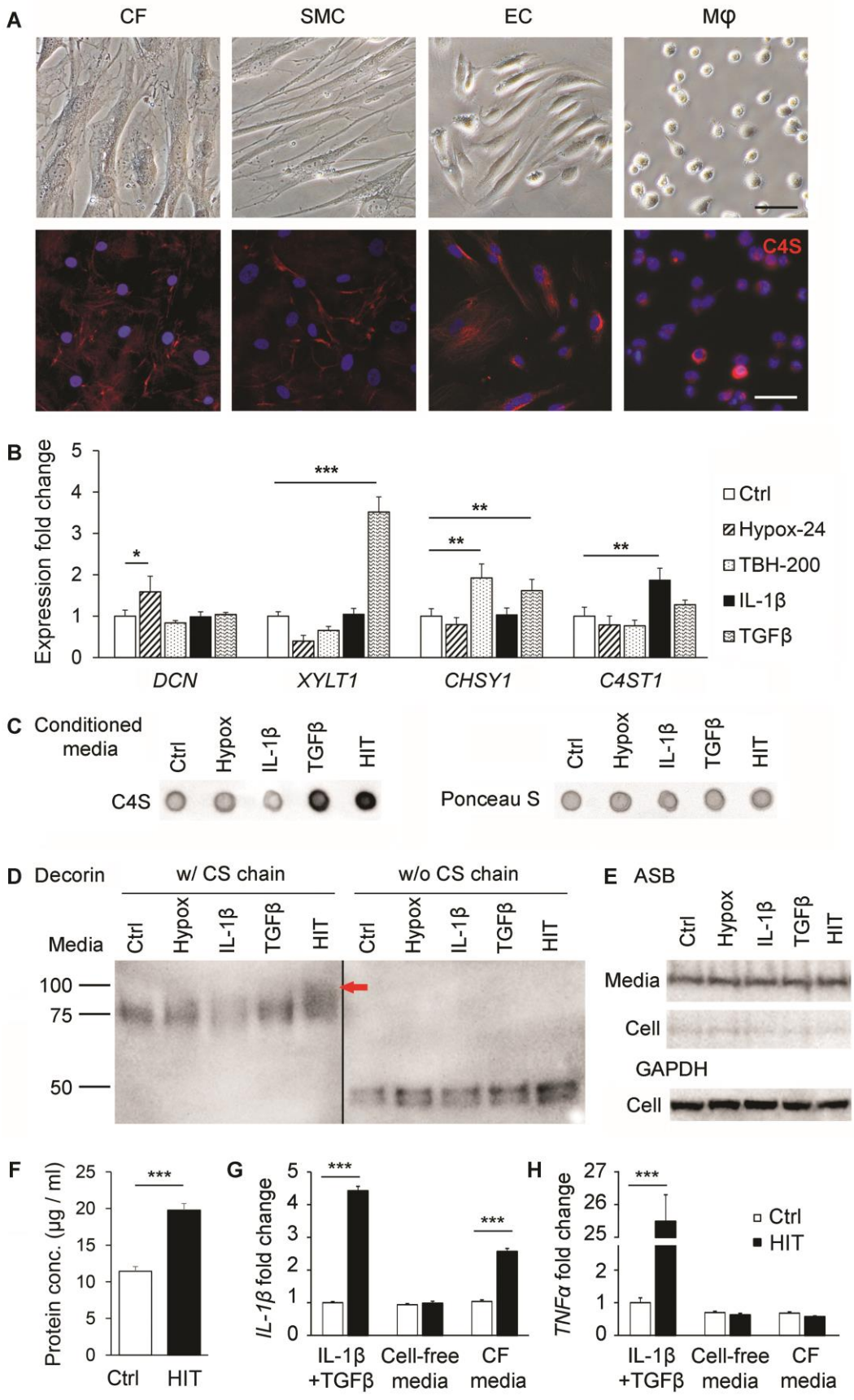

Figure 3. CSPG upregulation in primary human cardiac cells. (A) Bright field and C4S immunostained images of primary human cardiac fibroblasts (CF), endothelial cells (EC), smooth muscle cells (SMC), and THP-1 derived macrophages (Mφ), under basal conditions. Scale bar, 50 µm. **(B)** In CF, mRNA concentration of protein core (*DCN*) and enzymes for CS chain initiation (*XYLT1*), elongation (*CHSY1*), and sulfation (*C4ST1*) were upregulated by hypoxia, TGFβ, oxidative stress or TGFβ, and IL-1β respectively. Data is presented as mean ± SD. TBH, tert-butyl hydroperoxide. *$p<0.05$, **$p<0.01$, ***$p<0.001$ (One-way ANOVA followed by Tukey's post-hoc test). N=3. (C) Dot blot of CF conditioned media for C4S. Ponceau S stain of the same to confirm equal protein loading. TGFβ induced C4S increase, with further upregulation by the combined treatment with hypoxia, IL-1β and TGFβ ("HIT"). **(D)** Western blot for decorin (DCN), with or without CS chain, using CF conditioned media. Molecular weight (MW) of DCN with CS chain after "HIT" treatment was increased (red arrow), compared to any single treatment condition. **(E)** Western blot for ASB in CF conditioned media and in CF cell pellet lysate. GAPDH was used as loading control for cell pellet lysates. **(F)** Protein concentration of conditioned media collected from "HIT"-treated CF was significantly increased. **(G)** CF secreted high MW ECM proteins after "HIT" treatment which induced *IL1B* upregulation in macrophages. CF were treated with "HIT" conditions and the conditioned media was filtered with a 50 kD cut off membrane. The high MW portion (free of cytokines) was added to *in vitro* cultured macrophages. *IL1B* expression was significantly upregulated in macrophages (***$p<0.001$, right pair of data). Direct incubation with IL-1β and TGFβ into media also induced significant *IL1B* upregulation in macrophages (***$p<0.001$, left pair of data). Cell-free media treated with the same "HIT" conditions and filtered with 50 kD cut off membrane did not trigger *IL1B* changes when added into macrophage culture (middle pair of data). **(H)** *TNFA* expression in macrophages as in G. Unlike *IL1B*, CF conditioned media did not induce *TNFA* upregulation, while IL-1β and TGFβ cytokines significantly induced upregulation. N=3 for each experiment.

Disclaimer: The manuscript and its contents are confidential. Intended for journal review purposes only, and not to be further disclosed.

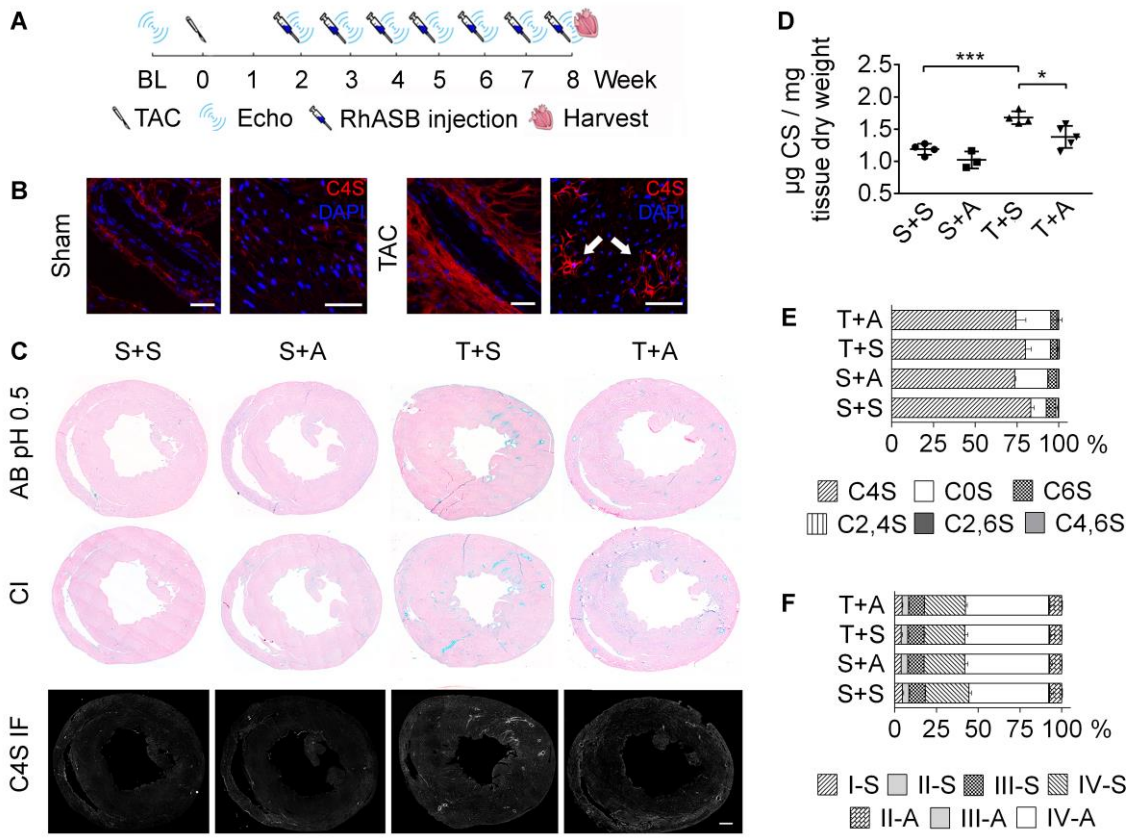

Figure 4. Myocardial C4S reduction following 7 weeks of systemic rhASB treatment *in vivo*. (A) *In vivo* experimental timeline. **(B)** C4S accumulation was found in perivascular space and interstitium in TAC rat hearts. Scale bar, 20 µm. (**C**) Rat cardiac sections from each of the sham+saline (S+S), sham+rhASB (S+A), TAC+saline (T+S) and TAC+rhASB (T+A) groups were stained with Alcian blue (AB) at pH 0.5 for sulfated GAGs (i.e. CS or HS), colloidal iron (CI) which stains for total mucin, or immunostaining with 2H6 monoclonal antibody that specifically recognizes C4S. **(D)** CS extracted from rat hearts quantified by Alcian blue assay. ***p<0.001, *p=0.022 (One-way ANOVA followed by Tukey's post-hoc test). **(E)** LCMS analysis of relative CS disaccharide composition. **(F)** LCMS analysis of relative HS disaccharide composition. No significant change was observed in either CS or HS between groups. N=4 for relative composition assays. I-S: ΔUA,2S-GlcNS,6S; II-S: ΔUA-GlcNS,6S; III-S: ΔUA,2S-GlcNS; IV-S: ΔUA-GlcNS; IV-A: ΔUA-GlcNAc; III-A: ΔUA,2S-GlcNAc; II-A: ΔUA-GlcNac,6S.

Disclaimer: The manuscript is confidential, intended for its only, and not to be furt

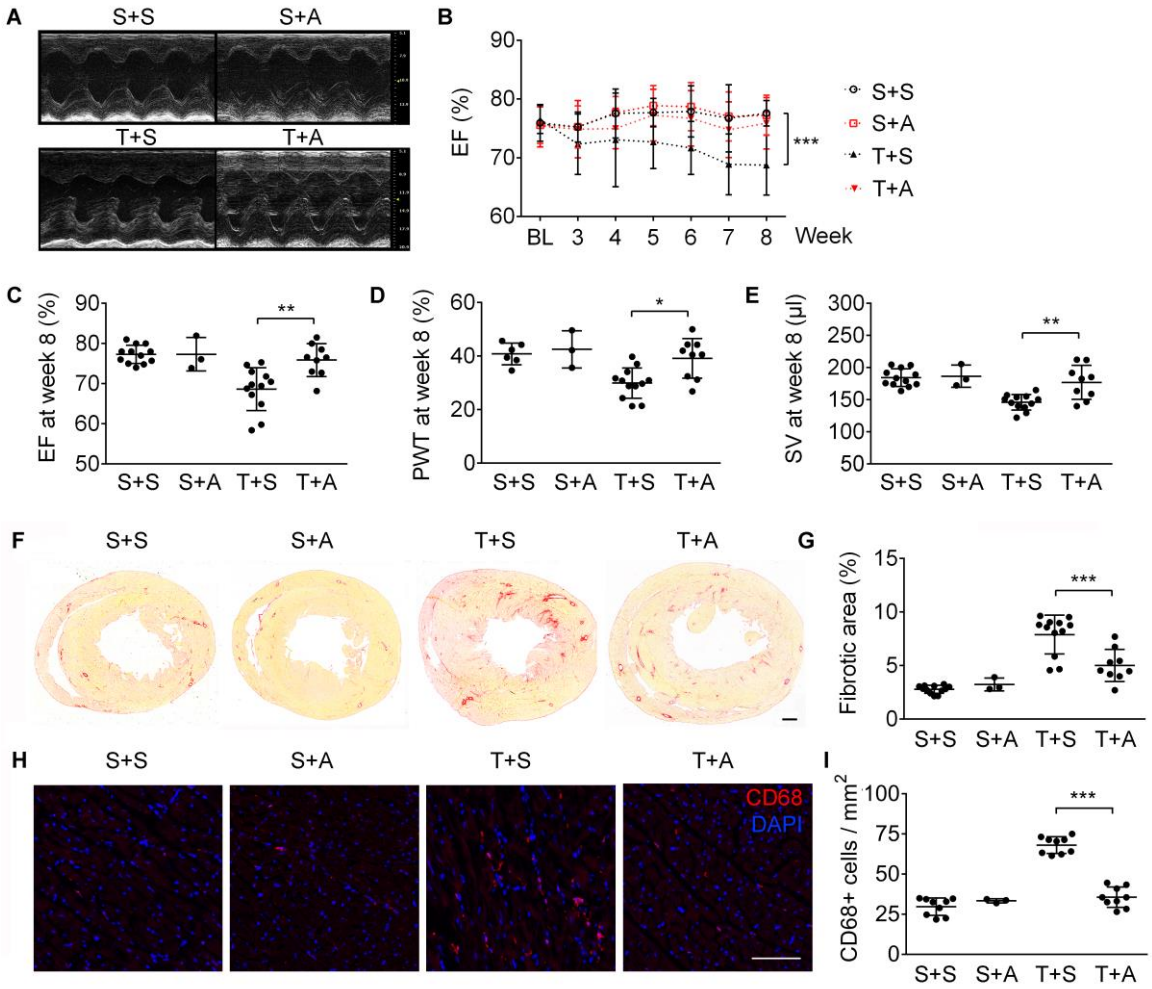

Figure 5. RhASB treatment *in vivo* prevents functional deterioration in TAC rats. (A) M-mode echocardiographic images of rat hearts 8 weeks post-TAC. S+S: Sham+saline, S+A: Sham+rhASB, T+S: TAC+saline, T+A: TAC+rhASB; group sizes were 12, 3, 12, 9 respectively. **(B)** Ejection fraction (%EF) measured over time. ***p<0.001 (Two-way ANOVA for repeated measures followed by Tukey's post-hoc test). **(C) %EF**, measured at week 9. Data presented as individual values and mean ± SD, **p=0.0019. One-way ANOVA followed by Tukey's post-hoc test. The same statistical method was applied for (D), (E), (G) and (I). **(D)** Percentage posterior wall thickening (%PWT) measured at week 8. *p=0.0105. **(E)** Stroke volume (SV) measured at week 8. **p=0.0018. **(F)** Myocardial fibrosis visualised by Sirius red (SR) staining. **(G)** Quantification of fibrosis as percentage SR positive area using ImageJ software. ***p<0.001. **(H)** Myocardial macrophages identified by immunostaining with CD68 antibody. Scale bar, 100 µm. **(I)** Macrophage cell count per section unit area (mm^2). ***p<0.001.

Disclaimer: The ma... confidential, intended ... only, and not to b...

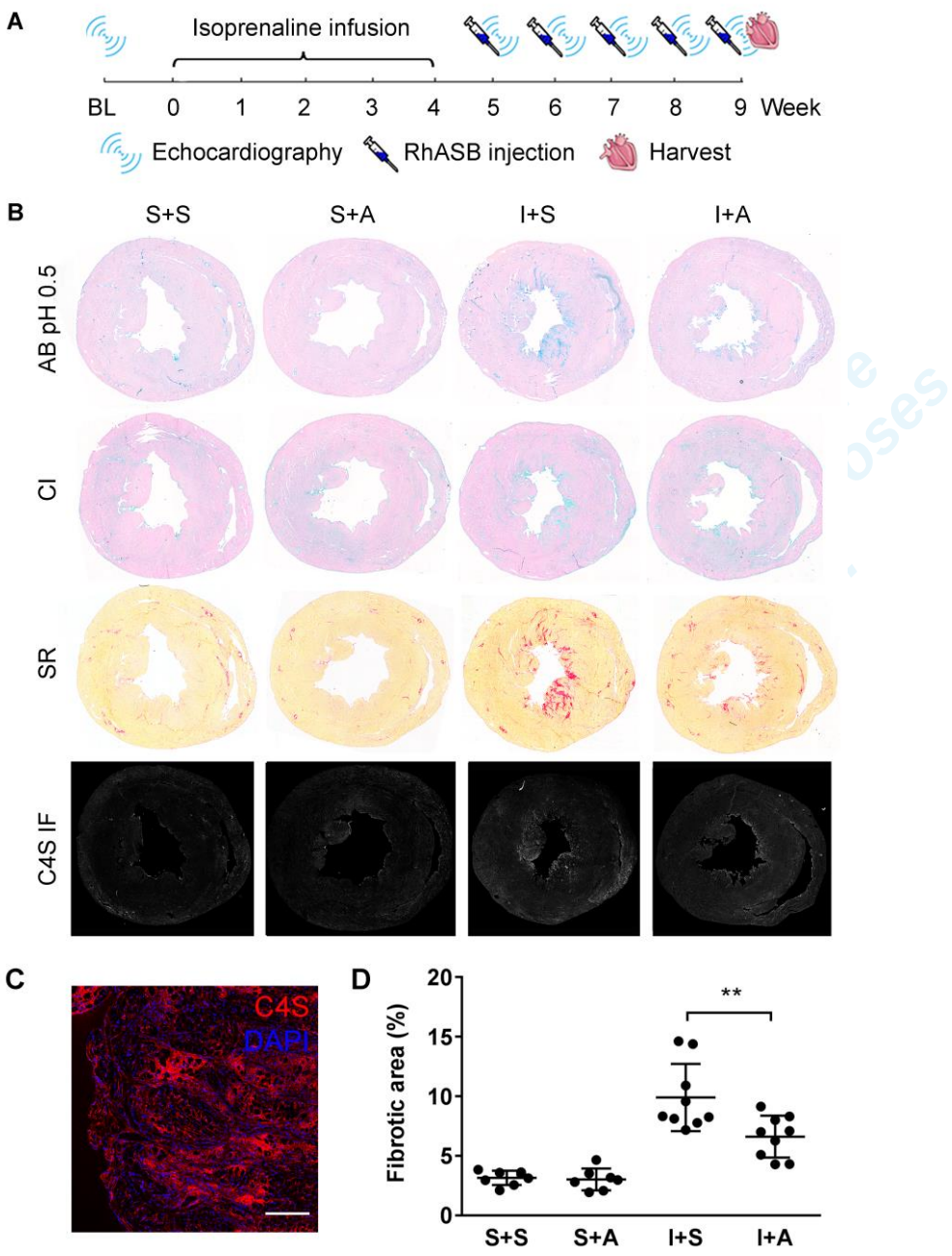

Figure 6. Isoprenaline treatment induced CS upregulation in rat hearts which was attenuated by rhASB treatment *in vivo*. (A) Experimental timeline for isoprenaline induced pathological remodeling model with delayed rhASB treatment. **(B)** Rat cardiac sections from each of the sham+saline (S+S), sham+rhASB (S+A), isoprenaline+saline (I+S) and isoprenaline+rhASB (I+A) groups were stained with Alcian blue (AB) at pH 0.5 for sulfated GAGs (i.e. CS or HS), colloidal iron (CI) which stains for total mucin, Sirius red (SR) for collagen, and immunofluorescent (IF) staining with the monoclonal antibody 2H6 which specifically recognizes C4S. (**C**) C4S precipitation pattern in a representative region of myocardial injury from an isoprenaline treated rat. Scale bar, 200 µm. (**D**)

Quantification of fibrosis as percentage SR positive area using ImageJ software. **p=0.009. One-way ANOVA followed by Tukey's post-hoc test

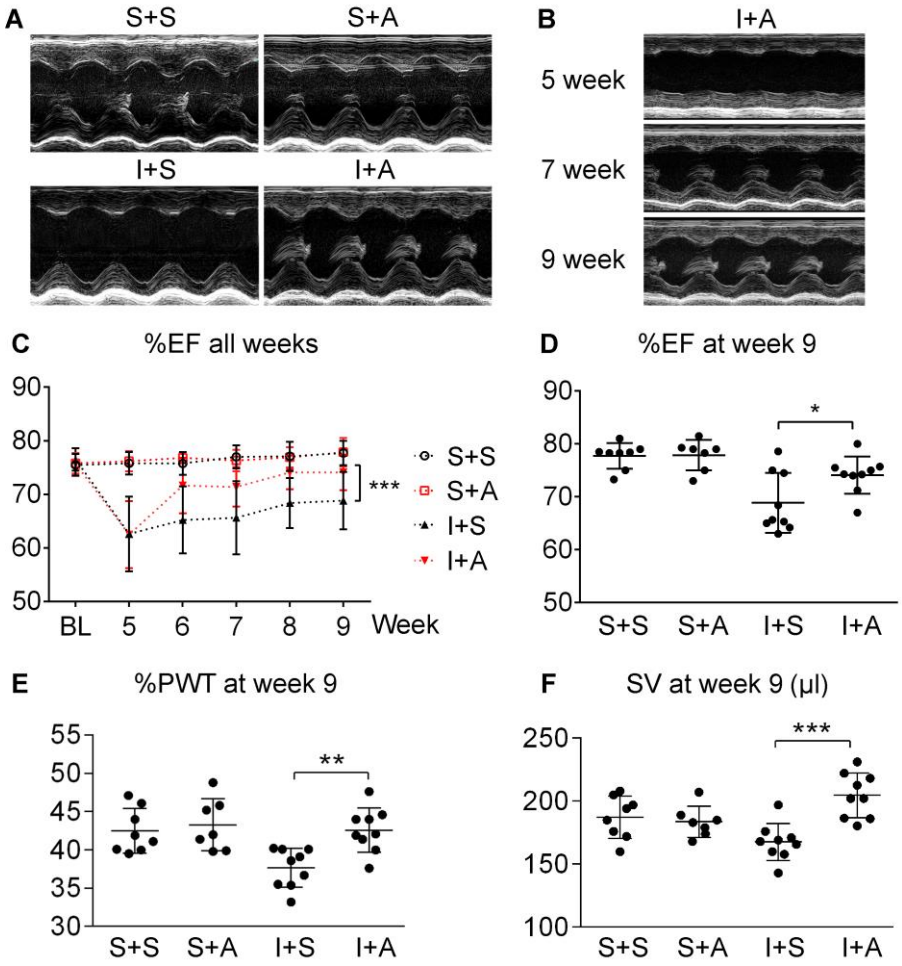

Figure 7. RhASB treatment *in vivo* improved functional recovery following isoprenaline induced pathological remodelling. (A) M-mode echocardiographic images of rat hearts at week 9. S+S, sham+saline, S+A, sham+rhASB; I+S, isoprenaline+saline, I+A, isoprenaline+rhASB, group sizes were N=8, 7, 9, 9 respectively. **(B)** Representative M-mode echocardiography from rats in group I+A at three time points during the treatment period. **(C)** Ejection fraction (%EF) measured over time. ***p<0.001 (Two-way ANOVA for repeated measures followed by Tukey's post-hoc test). **(D)** %EF measured at week 9. *p=0.039 (One-way ANOVA followed by Tukey's post-hoc test, data represented as individual values and mean ± SD. Same statistics method applies to (E-G)). **(E)** Percentage posterior wall thickening (%PWT): percentage change of wall thickness between diastole and systole, at week 9. **p=0.0065. **(F)** Stroke volume (SV) at week 9. ***p<0.001.

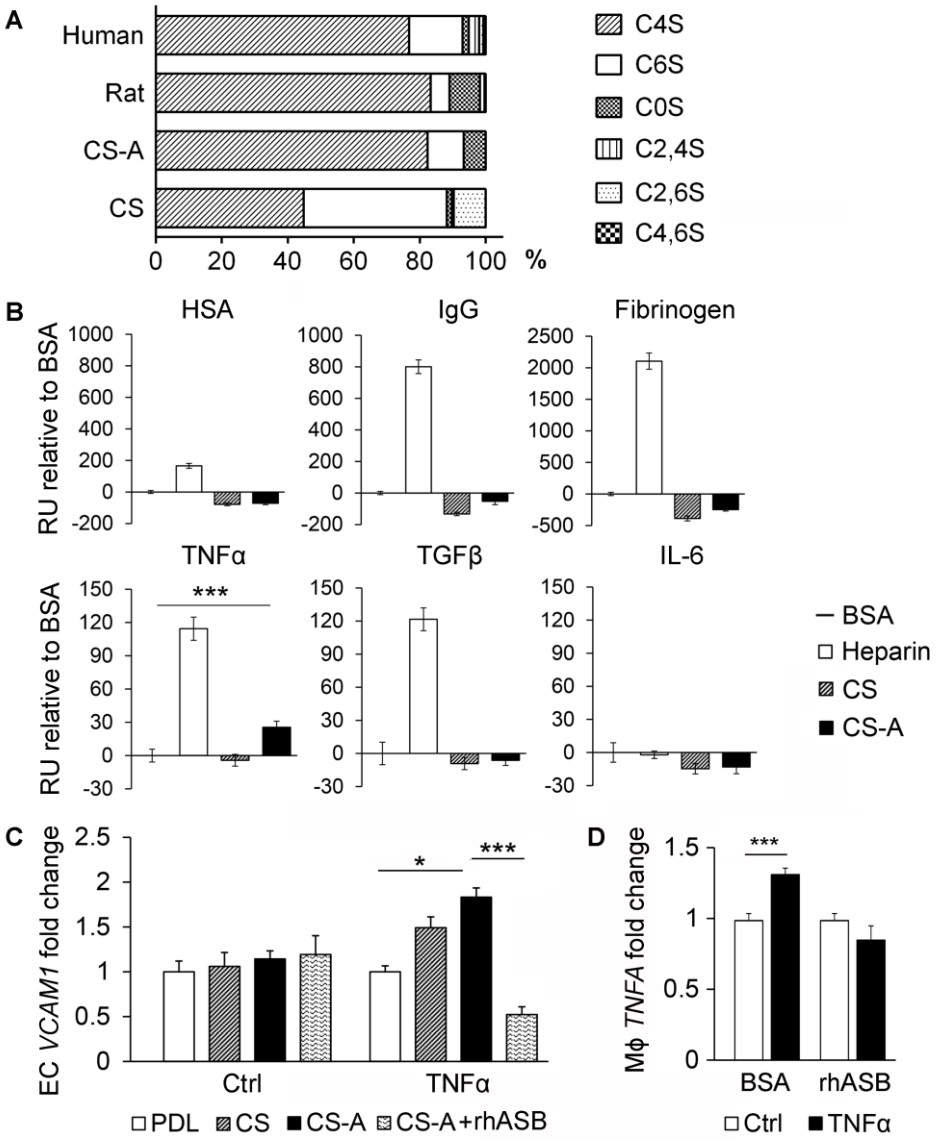

Figure 8. CS chain directly binds to and potentiates TNFα induced inflammation, which can be abolished by rhASB. (A) CS disaccharide relative composition determined by LCMS. CS-A composition resembled that of human and rat heart CS. **(B)** Binding strengths between GAGs and protein ligands measured using the XPR system. Response units (RU) were referenced to BSA. Heparin was used as positive control. CS-A showed positive binding to TNFα, but not to human serum albumin (HSA), IgG, fibrinogen, TGFβ or IL-6. ***p<0.001 (One-way ANOVA followed by Tukey's post-hoc test). **(C)** RT-qPCR of TNFα target gene *VCAM1* in CF cultured on poly-D-lysine (PDL), CS-A substrate, or CS-A+rhASB, pre-coated with or without TNFα. CS-A, but not PDL, bound TNFα to induce *VCAM1* expression. Pre-treatment of CS-A with rhASB abolished *VCAM1*

induction. Data are presented as mean ± SD; *p=0.0105, ***p<0.001, (One-way ANOVA followed by Tukey's post-hoc test). N=3 for each assay. **(D)** THP-1 derived macrophages showed *TNFA* upregulation when activated by TNFα on pre-bound CS-A substrate. The effect was blocked by pre-treating CS-A with rhASB, but not BSA. ***p<0.001 (Student's t-test), N=3 in each group.

Disclaimer: The manuscript and its contents are confidential, intended for journal review purposes only, and not to be further disclosed.